Soft Computing
https://doi.org/10.1007/s00500-020-05199-7

METHODOLOGIES AND APPLICATION

Short-term photovoltaic power generation predicting by input/output structure of weather forecast using deep learning

Dongha Shin[1] · Eungyu Ha[1] · Taeoh Kim[1] · Changbok Kim[1]

Abstract
In Korea, weather forecasts for fundamental weather factors, such as temperature, precipitation, wind direction and speed, humidity, and cloudiness, are provided for a three-day period in each region. This can facilitate predicting photovoltaic power generation based on weather forecasting. For this purpose, in the present paper, we aim to propose corresponding model. However, the Korea Meteorological Administration does not forecast the amount of solar radiation and sunshine that mostly influence the results of photovoltaic power generation prediction. In this study, we predict these parameters considering various input/output (I/O) variables and learning algorithms applied to weather forecasts on hourly weather data. Finally, we predict photovoltaic power generation based on the best sunshine and solar radiation prediction results. The data structure underlying all predictions relies on four models applied to fundamental weather factors on sunshine and solar radiation data two hours ago. Then, the photovoltaic power generation prediction is implemented using four models depending on whether to add the predicted sunshine and solar radiation data obtained at the previous step. The prediction algorithm relies on an adaptive neuro-fuzzy inference system and artificial neural network (ANN) techniques, including dynamic neural network (DNN), recurrent neural network (RNN), and long short-term memory (LSTM). The results of the conducted experiment indicate that ANN perform better than the neuro-fuzzy approach. Moreover, we demonstrate that RNN and LSTM are more suitable for the time series data structures compared with DNN. Furthermore, we report that the weather forecast structure and the model 4 structure, which includes sunshine and solar radiation data two hours ago, achieve the best prediction results.

Keywords Photovoltaic · Meteorological factors · Power generation predicting · Artificial neural network · Adaptive neuro-fuzzy inference system

1 Introduction

In recent years, the question of reducing the consumption of fossil fuels has been widely considered, as they constitute one of the main causes of resource depletion and global warming. The countries that expend the large amounts of fossil fuels need to address this problem. One of the possible ways is the implementation of photovoltaic power generation that is infinite, environmentally friendly, and evenly distributed compared to fossil fuels. However, the initial investments and the unit costs associated with power generation are high and the installation sites are limited. Large installation areas are required due to low energy density. Accordingly, it is difficult to predict the amount of power generation, as it largely depends on weather conditions. Therefore, it is difficult to control and establish advanced plans. To resolve this problem, it is necessary to decrease the uncertainty associated with power generation and to introduce highly accurate power generation predicting technologies (Lee 2017; Rhee et al. 2011).

Concerning solar power generation, it is possible to consider short-term predicts with a time unit, midterm predicts with a day unit, and long-term predicts with a week or a

Communicated by V. Loia.

✉ Changbok Kim
cbkim@gachon.ac.kr

Dongha Shin
aquinasdh0129@gmail.com

Eungyu Ha
dmsrbx97@gmail.com

Taeoh Kim
tokim98@naver.com

[1] Gachon University, Seongnam-daero, Sujeong-gu, Seongnam-si, Gyeonggi-do 13120, Korea

Published online: 23 September 2020

month unit (Giebel et al. 2011; Lei et al. 2009; Costa et al. 2008; Mirasgedis et al. 2006; Hong et al. 2014).

The short-term predicts can be applied to operate a power plant effectively and connect reliably with other electric systems. Long-term predictions can be used to evaluate power generation profits and establish investment plans; however, photovoltaic power plants require large initial investments. The short-term predict model can be developed to predict power generation in a real-time manner or for the subsequent 24 hours (Welch et al. 2009).

Photovoltaic power generation prediction methods include the physical modeling, statistical, and probabilistic approaches. Prediction algorithms that have been researched at present rely on wavelet theory, autoregressive integrated moving average, extreme learning machine, support vector regression, neuro-fuzzy networks, and artificial neural networks (ANNs) (Conejo et al. 2005; Lee et al. 2015; Cha et al. 2014; Lee and Ji 2015; Lee and Lee 2016; Yona et al. 2013). Machine learning is a core technology in the field of big data that enables computers to acquire intelligence by learning the relevant data. Deep learning is a machine learning technique that imitates the human brain structure. It has improved the capabilities of the existing ANNs and can be implemented in a variety of areas, including image recognition, voice recognition, natural language processing, and future prediction (Bengio 2009; Deng and Yu 2014; LeCun et al. 2015).

In the present study, we proposed a short-term model using the hourly weather data from the Mokpo Meteorological Administration and the time-based power generation data obtained from Yeongam solar power plants from the period 2013–2015. The meteorological data comprise the information about various meteorological factors such as temperature, precipitation, wind direction and speed, humidity, and cloudiness registered by the Mokpo Meteorological Administration near the Yeongam solar power plants.

As the Korea Meteorological Administration does not forecast the amount of sunshine and solar radiation, which are the important weather factors in solar power generation prediction. Additionally, power generation data were obtained from the least error model. Furthermore, the weather data can be predicted using the I/O structure of four models. Model 1 is realized for predicting power generation and can be established using only the fundamental weather data. Model 2 includes sunshine data registered during the previous two hours, based on the current time. Model 3 includes the solar radiation data of the previous two hours, based on the current time. Model 4 incorporates the sunshine and solar radiation data of the previous two hours, according to the current time.

The prediction algorithm proposed in the present study relies on the adaptive neuro-fuzzy inference system (ANFIS), a general structure of the neuro-fuzzy technique, as well as on ANNs, including a dynamic neural network (DNN), recurrent neural network (RNN), and long short-term memory (LSTM). ANFIS is realized in MATLAB and Simulink, and ANNs are implemented in a deep learning network using TensorFlow.

Table 1 Correlation between major meteorological factors and power generation

	24-hr data	12-hr data	7-hr data	Day data
Temperature	0.243	0.259	0.182	0.188
Precipitation	−0.071	−0.118	−0.178	−0.398
Wind direction	0.23	0.216	0.191	0.222
Wind speed	0.231	0.169	0.111	−0.054
Humidity	−0.607	−0.595	−0.624	−0.449
Cloudiness	−0.251	−0.441	−0.73	−0.801
Sunshine	0.957	0.935	0.877	0.918
Solar radiation	0.851	0.766	0.804	0.922

2 Meteorological factors and prediction algorithm

2.1 Meteorological factors

Photovoltaics produce electricity accumulating the radiation energy of the sun. Therefore, electric light, solar radiation, and sunshine are considered as important factor in the prediction of power generation. As photovoltaics are semiconductors, it is necessary to ensure a suitable temperature and humidity. Considering that most meteorological factors largely impact the results of photovoltaic power generation, the power generation amount is intermittent, depending on the current weather conditions. Therefore, an efficient power generation prediction technology incorporating meteorological factors is required to reduce uncertainties and to improve the economy of solar power generation. Table 1 represents the correlation between meteorological factors and solar power generation.

The weather data are obtained from the Mokpo Meteorological Administration and cover the period of 2013–2015. The photovoltaic power generation data are provided the power plant in Yeongam, South Jeolla Province. The 24-hr data correspond to the whole hourly data per day; the 12-hr data are the hour data from 07:00 to 18:00; and the 7-hr data are the hour data from 10:00 to 16:00, representing more than 90% of daily power generation. Moreover, the daily data are defined as the average data per day. Cloudiness is expected to be highly correlated with power generation, as it is primarily related to the amount of sunshine and solar radiation. However, considering that the 24-hr data do not comprise power generation between sunset and sunrise, regardless of cloudiness, the correlation is rather low (−0.251). The

12-hr data demonstrate high correlation, because the data between sunset and sunrise were deleted. The interrelation with cloudiness has increased more than twice. However, that of solar radiation and sunshine slightly decreased. The 7-hr data correlation coefficient of cloudiness has been found equal to −0.73, which is three times higher than that of the 24-hr data. Concerning the day data, the daily data from the Mokpo Meteorological Administration for meteorological factor are utilized, except for cloudiness. Specifically, to incorporate cloudiness, we consider the average data for the period between 07:00 and 18:00 during which the solar power generator runs. The daily data demonstrate greater correlation with cloudiness, sunshine, and solar radiation that are important meteorological factors in the prediction of solar power generation compared with the hourly data. However, it should be noted that the hourly data are more refined compared with day data in the prediction of power generation using meteorological data. In this study, 24-hr data are tested using DNN1, 12-hr data with DNN2, and 7-hr data with DNN3.

2.2 Prediction algorithm

The neuro-fuzzy system combines the learning ability of an artificial neural network and the human knowledge expression of a fuzzy system. The system structure includes an input layer in which the original data are inputted, a hidden layer to learn fuzzy parameters, and an output layer to generate the predicted results. Each input layer transmits an external crisp signal to the next layer. The hidden layer consists of the fuzzification, the fuzzy rule, the output membership, and the defuzzification layers. The ANFIS is defined as artificial neural network model that functions the same as Sugeno fuzzy inference model. The fuzzy rules are formulated in the form of the linear combinations of consequent and antecedent (Thangaramya et al. 2019; Priya et al. 2014; El-kader and Elshora 2020; Yu and Kim 2016).

$$R^j : X_{1j}\ is\ A_{1j}\ AND\ X_{2j}\ is\ A_{2j} \ldots AND\ X_{nj}\ is\ A_{nj}$$
$$then$$
$$y = f = a_{0j} + a_{1j}X_{1j} + a_{2j}X_{2j} + \cdots + a_{nj}X_{nj} \quad (1)$$

where i is the number of inputs; j is the number of rules; and X_i and y are the input and output variables. Moreover, A_{ij} is a linguistic term with $u_{A_{ij}}(X)$, and $a_{ij} \in R$ is the coefficient of linear equation $f_j = (X_1, X_2, X_3 \ldots X_n)$. If there are two input variables (X_1, X_2), one output (y), and two fuzzy rules, the following can be written.

$$R^1 : X_1\ is\ A_{1^1}\ AND\ X_2\ is\ A_{2^1}\ then$$
$$y = f_1 = a_{0^1} + a_{1^1}X_1 + a_{2^1}X_2 \quad (2)$$
$$R^2 : X_1\ is\ A_{1^2}\ AND\ X_2\ is\ A_{2^2}\ then$$

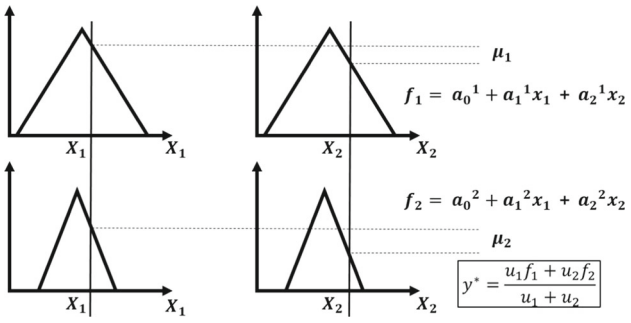

Fig. 1 ANFIS at two inputs and one output

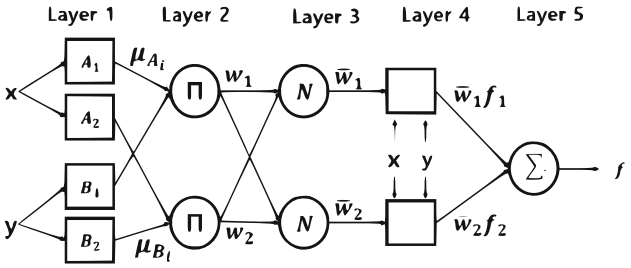

Fig. 2 ANFIS structure

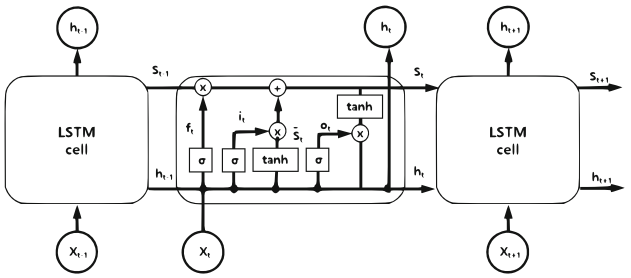

Fig. 3 LSTM Strucutre

$$y = f_1 = a_{0^2} + a_{1^2}X_1 + a_{2^2}X_2 \quad (3)$$
$$y^* = \frac{u_1 f_1 + u_2 f_2}{u_1 + u_2} \quad (4)$$

Figure 1 represents fuzzy operation at two inputs and one output. Figure 2 outlines the ANFIS structure.

Layer 1 corresponds to the membership function $u_{A_{ij}}(X_i)$ belonging to the input. It generates the compatibility for input X_i of A_{ij}. A membership function usually employs the bell curve function. Layer 2 is outputted as the weight multiplied by the output of layer 1. It indicates the compatibility of the fuzzy rule. Layer 3 computes the normalized compatibility of fuzzy rules. That is, the jth node corresponds to a value obtained by dividing the compatibility of the jth fuzzy rule by the sum of all compatibility estimates. Layer 4 outputs the normalized value and the product of conclusion. Layer 5 combines the outputs of the Layer 4 to obtain an inference

Table 2 ANFIS parameter setting

Parameter	Configuration of ANFIS	
	Experiment 1	Experiment 2
Number of nodes	471	471
Number of linear parameters	216	216
Number of nonlinear parameters	45	45
Total number of parameters	261	261
Number of training data pairs	6552	17520
Number of checking data pairs	0	0
Number of fuzzy rules	216	216

value for the entire system as follows:

$$o_i^1 = \begin{cases} u_{A_i}(x) = \exp\left(-\frac{1}{2}\left(\frac{x-m_i}{\sigma}\right)^2\right) \\ u_{B_i}(y) = \exp\left(-\frac{1}{2}\left(\frac{y-m_i}{\sigma}\right)^2\right) \end{cases} \tag{5}$$

$$o_i^2 = w_1 = \mu_{A_i}(x) X \mu_{B_i}(y) \tag{6}$$

$$o_i^3 = \bar{w}_l = \frac{w_1}{w_1 + w_2} \tag{7}$$

$$o_i^4 = \bar{w}_l f_i = \bar{w}_l (p_i x + q_i \mu + r_i) \tag{8}$$

$$o_i^5 = \mu_i^* = \sum_{i=1}^{2} \bar{w}_l f_i = \sum_{i=1}^{2} \frac{\sum w_i f_i}{\sum w_i} \tag{9}$$

where m_{ij} and σ_{ij} are the learning parameters that represent the mean and standard deviation in the center and width of the function, respectively; p_i, q_i and r_i are the parameters to be learned and are referred to as the consequent parameters.

Artificial intelligence is a core area underlying the concept of machine learning that is aimed at enabling computers to imitate the intelligent behavior of humans. ANNs were developed and then advanced to the deep learning methods, such as DNN, RNN, and LSTM, including reinforcement learning. They can be applied to all areas of human activities, including image recognition, voice recognition, natural language processing, and future prediction (LeCun et al. 2015). DNN is used to solve the weight initialization problem using the corresponding technique and deepening the hidden layer through the dropout method that removes the hidden layer node to prevent overfitting. DNN employs the ReLu and tanh activation functions to solve the gradient vanishing, a problem with sigmoid active functions:

$$\text{actReLu}(x) = \max(0 : x) \tag{10}$$

$$\text{acttanh}(x) = \tanh(x) \tag{11}$$

The sigmoid function has a maximum value of 1 and a minimum value of 0 so that the derivative value converges to 0. Accordingly, the derivative value disappears when learning is performed on more than three layers. Furthermore, as the center value of the function is not 0, learning can be slow due to a large amount calculation. The tanh function can be used to eliminate the disadvantage of slow learning by reducing the amount of computation through setting the center value zero. However, the problem of the derivative value converging to 0 is not resolved. As the ReLu function is a straight line with the slope of 1 when x > 0 and 0 when x < 0, the negative part is eliminated so that learning is faster than the above two functions. Moreover, due to the characteristics of a straight line with the slope of 1, the computational cost is not large, and implementation is simple.

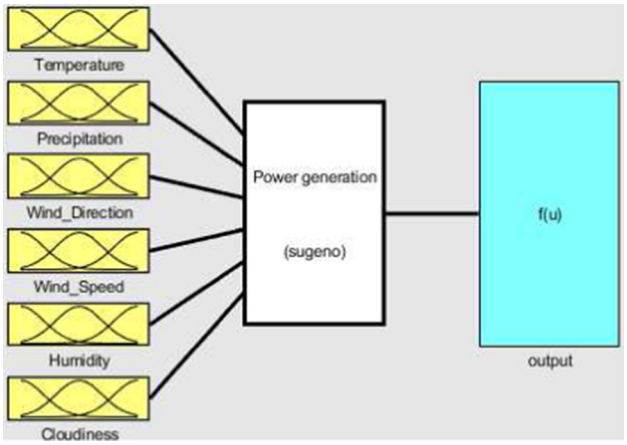

Fig. 4 ANFIS structure in MATLAB/Simulink

RNN forms parallel chain connections with DNN having one common input and output patterns. It uses past learning results for current learning and is effective for processing time series data. RNN is associated with the long-term dependence problem, meaning that the past learning results disappear when a chain becomes long. LSTM can be used to solve the long-term dependence problem by using a structure that delivers past learning results of cells without considerable changes through a cell state that is maintained through the entire chain (Goodfellow et al. 2016; Kim et al. 2016). In the first step, LSTM determines the information to delete. In the second step, it decides whether to save new information in the cell sate. In the third step, it updates the cell state.

Table 3 Neural network parameter setting

Parameter	Configuration	
	DNN	RNN-LSTM
Number of input nodes	Number of input factors	Number of input factors
Number of hidden layer nodes	32	32
Number of hidden layers	3	/
Number of output node	1	1
Time stamp	/	12, 24, 48
Learning rate	0.01	0.01
Number of iterations	15000	5000

Lastly, it determines the value to output. Figure 3 presents the LSTM structure.

$$f_t = \sigma(W_f \cdot |h_{t-1}, x_t + b_f) \tag{12}$$
$$i_t = \sigma(W_f \cdot |h_{t-i}, x_t + b_i) \tag{13}$$
$$\check{S}_t = \tanh(W_s \cdot |h_{t-1}, x_t + b_s) \tag{14}$$
$$S_t = f_t * S_{t-1} + \check{S}_t \tag{15}$$
$$o_t = \sigma(W_o \cdot |h_{t-i}, x_t + b_o) \tag{16}$$
$$h_t = o_t * \tanh(S_t) \tag{17}$$

Here, f_t is the output of the first step; i_t and $\check{S}_t$ are the outputs of the second step; S_t is the output of the third step; o_t and h_t are the outputs of the last step; W denotes weight, b is bias; and t indicates time tamp.

2.3 Algorithm performance evaluation

In the present study, to evaluate the prediction results of ANFIS, DNN, RNN, and LSTM, the power generation predicted values are compared considering weather factors, such as temperature, precipitation, humidity, wind speed and direction, and cloudiness. Table 2 represents ANFIS parameter setting. Figure 4 outlines ANFIS structure composed in MATLAB.

Table 3 presents the deep learning parameters setting.

The numbers of the input and output nodes in DNN are identical to the numbers of input variables and labels of the input and output model. The hidden layers include of 32 nodes in three layers. Furthermore, the ReLu and tanh activation functions are utilized, and the learning process is repeated 15,000 times at the learning rate of 0.01.

The number of the input and output nodes of RNN-LSTM are identical to the number of input variables and labels in the I/O model. The hidden layers are composed of 32 nodes. Furthermore, the ReLu and tanh activation functions are used similarly as DNN, and the learning process is repeated 5,000 times at the learning rate of 0.01. As the meteorological and power data have similar patterns in one-day intervals, the RNN-LSTM cells are configured using 12, 24, and 48 time stamps for learning in a day unit.

Table 4 RMSE of power generation prediction using weather factors with all considered algorithms

	Experiment 1	Experiment 2
ANFIS	0.207	0.204
DNN	0.204	0.195
RNN	0.13	0.105
LSTM	0.121	0.1

To compare ANFIS and ANN, fundamental weather factors such as temperature, precipitation, wind speed and direction, humidity, and cloudiness were used.

Algorithm comparing model is for predicting the sunshine and solar radiation one hour later using the basic meteorological factors of the present time. The first experiment was conducted using the data from January to September 2015 as the training data and from October to December 2015 as the test data. The second experiment was based on the data from 2013 to 2014 as the training data, and the data for 2015 were used as the test data. The algorithms mentioned in the present paper in the Table 4 were compared and evaluated using in terms of the root mean square error (RMSE).

In Experiment 1, ANFIS demonstrated RMSE of 0.207; DNN showed RMSE of 0.204; RNN reached RMSE of 0.13. LSTM achieved RMSE of 0.121. Therefore, we concluded that LSTM showed the best predicting results. The RMSE of LSTM was 1.71 times better than that of ANFIS. In Experiment 2, ANFIS showed RMSE of 0.204; DNN reached RMSE of 0.195; RNN demonstrated RMSE of 0.105; LSTM showed RMSE of 0.1. Accordingly, LSTM showed the best predicting results as well. RMSE of LSTM was 2.04 times better than that of ANFIS. As a result of the conducted experiments, we confirmed that the prediction rate of ANNs was higher than that of the neuro-fuzzy method. Therefore, in this paper, we proposed a power generation prediction using ANNs: DNN, RNN, and LSTM. The experiment value was used as the average one by repeating the experiments for five times.

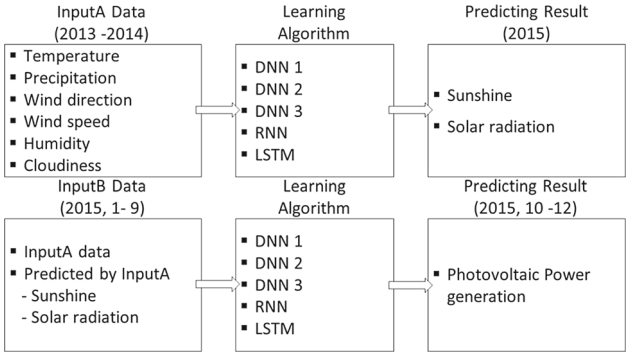

Fig. 5 Overall configuration for solar power generation predicting

3 Solar power predicting model

The supervised learning algorithms can achieve high accuracy by establishing highly relevant input variables with the labels corresponding to the output variables. Proposing an I/O model used in supervised learning is the most important factor in predicting. However, supervised learning requires a direct decision by humans through repeated experiments. As prediction using a neural network utilizes back propagation, the accuracy may vary according to the composition of the input and output variables used for prediction.

In Korea, weather forecasts for temperature, precipitation, wind direction and speed, humidity, and cloudiness are provided for a three-day period in each region. However, the Korea Meteorological Administration does not forecast the amount of solar radiation and sunshine that mostly influence the results of photovoltaic power generation prediction. In this study, we aimed to predict sunshine and solar radiation using various I/O variables and learning algorithms according to weather forecasts using hourly weather data and power generation data. Furthermore, photovoltaic power generation is predicted based on the best sunshine and solar radiation prediction results. Figure 5 represents the overall configuration for the proposed solar power generation predicting approach.

The learning data for predicting sunshine and solar radiation are the meteorological data for the period 2013–2014, and the test data are the meteorological data for 2015. The learning data for predicting power generation are meteorological data for the period January–September 2015, and the test data are the meteorological data for the period October–December 2015. The I/O factors are temperature (A), precipitation (B), wind direction (C), wind speed (D), humidity (E), cloudiness (F), sunshine (G), and solar radiation (H) data. Furthermore, to predict sunshine and solar radiation, we utilize the four models. Table 5 represents the data structure used to predict sunshine and solar radiation without weather forecast.

Table 5 Without weather forecast I/O structure

Model	Input variable							Label
	A-F	G2	G1	G0	H2	H1	H0	G,H
Model1	0	/	/	/	/	/	/	1
Model2	0	/	/	0	/	/	0	1
Model3	0	/	−1	0	/	−1	0	1
Model4	0	−2	−1	0	−2	−1	0	1

Table 6 Weather forecast I/O structure

Model	Input variable							Label
	A-F	G2	G1	G0	H2	H1	H0	G,H
Model1	1	/	/	/	/	/	/	1
Model2	1	/	/	0	/	/	0	1
Model3	1	/	−1	0	/	−1	0	1
Model4	1	−2	−1	0	−2	−1	0	1

Table 7 Without weather forecast I/O structure

Model	Input variable							Label
	A-F	G2	G1	G0	H2	H1	H0	I
Model1	0	/	/	/	/	/	/	1
Model2	0	−2	−1	0	/	/	/	1
Model3	0	/	/	/	−2	−1	0	1
Model4	0	−2	−1	0	−2	−1	0	1

The numbers in Table 5 represent time, with 0 being the present time. Model 1 is intended for predicting sunshine and solar radiation one hour later using the basic meteorological factors of the present time. Then, Model 2 adds the current sunshine and solar radiation factors to Model 1, Model 3 additionally incorporates the factors of sunshine and solar radiation one hour earlier than Model 2, and finally, Model 4 adds the factors of sunshine and solar radiation obtained two hours before Model 3. The label that serves as the output variable is defined as the sunshine and solar radiation data one hour later. Table 6 represents the I/O structure for predicting sunshine and solar radiation using weather forecasts.

Weather forecast I/O structure adopt the fundamental weather data one hour later to use weather forecasts data. It is as same as with Without weather forecast I/O structure with sunshine and solar radiation data. Tables 7 and 8 represent the I/O model to predict power generation.

Without weather forecast I/O structure is the typical prediction model which is used in comparing prediction algorithms. This structure for solar power generation prediction based on the data corresponding to the current time considers basic meteorological factors as the input and the one hour later solar power generation data as the output. Furthermore, an I/O structure for the weather forecast utilizes the predicted data one hour later as the input into the basic meteorological

Table 8 Weather forecast I/O structure

Model	Input variable							Label
	A-F	G2	G1	G0	H2	H1	H0	I
Model1	1	/	/	/	/	/	/	1
Model2	1	−2	−1	0	/	/	/	1
Model3	1	/	/	/	−2	−1	0	1
Model4	1	−2	−1	0	−2	−1	0	1

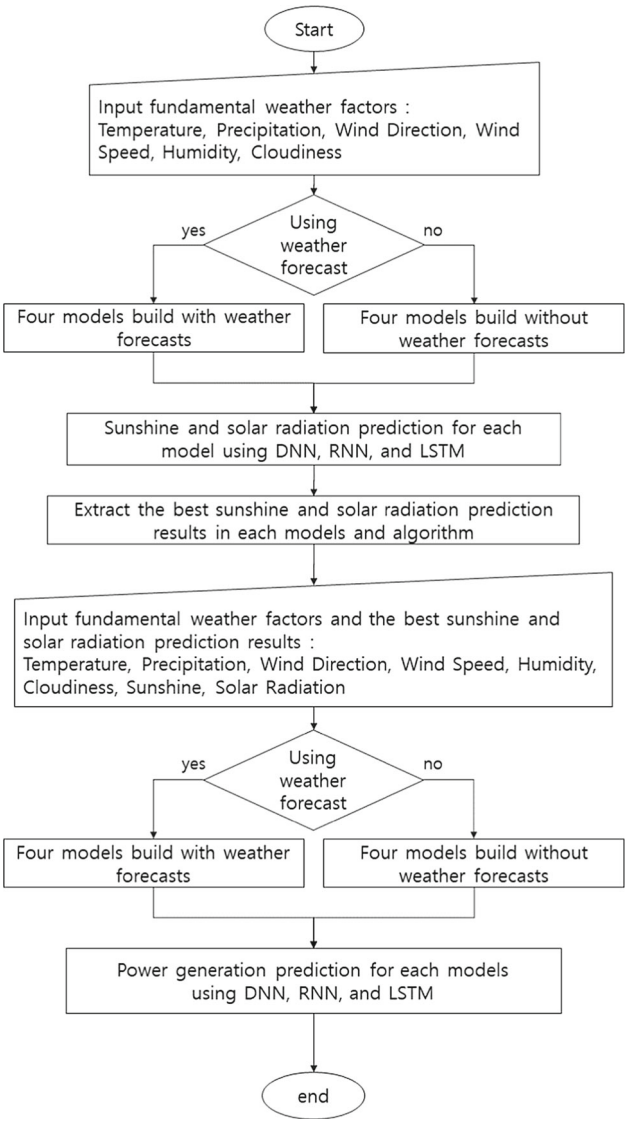

Fig. 6 Flowchart for solar power generation predicting

factors and the solar power generation data one hour later as the output. Model 1 predicts power generation using meteorological factors only; Model 2 uses the predicted sunshine data; Model 3 utilizes the predicted solar radiation data; and Model 4 employs the predicted sunshine and solar radiation data. Figure 6 represents a flowchart for the proposed solar power generation forecasting approach.

4 Experiments

The experimental environment was implemented using Windows 10 and TensorFlow GPU based on Python 3.6. The learning data for the sunshine and solar radiation predicting comprised 17,520 records for the period of 2013-2014. The test data comprised 8,760 records for 2015. The learning data used to estimate solar power generation were considered in the period January–September 2015, and the test data were used for the period of October–December. The meteorological factors had the different sizes of data, and therefore, the range of data had to be aligned. All meteorological factors were normalized between 0 and 1, as the I/O data used in ANN were effective for learning due to its small size.

$$\text{Normalization} = \frac{x_i - \min(x)}{\max(x) - \min(x)} \tag{18}$$

The RMSE, mean absolute error (MAE), correlation, and bias were considered to estimate the prediction accuracy and predicting results. The correlation served as a measure for evaluating the similarity between the predicted and actual values. If RMSE >> MAE, it meant that the predicted value exhibited a large deviation from the actual one. If RMSE was similar to MAE, it indicated that the predicted value had a small deviation from the actual value. Bias could be used to determine whether the predicted value was greater or smaller than the actual one. Correlation was considered to measure the similarity between the predicted and actual values:

$$\text{RMSE}(x', x) = \frac{1}{N}\sqrt{\sum_{n=1}^{N}(x_n{}' - x_n)} \tag{19}$$

$$\text{MAE}(x', x) = \frac{1}{N}\sum_{n=1}^{N}|x_n{}' - x_n| \tag{20}$$

$$\text{BIAS}(x', x) = \frac{1}{N}\sum_{n=1}^{N}(x_n{}' - x_n) \tag{21}$$

$$\text{COR.}(x', x) = \frac{\sum_{n=1}^{N}(x_n{}' - \bar{x'}) * \sum_{n=1}^{N}(x_n - \bar{x})}{\sqrt{\sum_{n=1}^{N}(x_n{}' - \bar{x'})^2 * \sum_{n=1}^{N}(x_n - \bar{x})^2}} \tag{22}$$

Table 9 presents the results of sunshine prediction. Here, all experimental results are averaged after five iterations. In Table 9, the gray area indicates the best result for each model. DNN1, DNN2, and DNN3 are the results of the 24-hr, 12-hr, and 7-hr of data, respectively. The experimental results indicated that the I/O structure using the weather forecasts achieved more accurate outcomes, and RNN-LSTM was better than DNN.

As represented in the above table, the predicting results corresponding to sunshine and solar radiation in the I/O structure incorporating weather forecasts were mostly acceptable.

Table 9 Predicting results of sunshine

		Without weather forecast I/O structure					Weather forecast I/O structure				
		DNN1	DNN2	DNN3	RNN	LSTM	DNN1	DNN2	DNN3	RNN	LSTM
Model1	RMSE	0.303	0.284	0.245	0.196	0.192	0.269	0.251	0.180	0.168	**0.167**
	MAE	0.210	0.200	0.159	0.12	0.107	0.181	0.164	0.106	0.099	**0.091**
	COR	0.640	0.727	0.790	0.867	0.875	0.736	0.796	0.892	0.903	**0.906**
	BIAS	0.018	-0.005	−0.019	0.014	−0.009	0.041	0.019	−0.005	−0.001	**0.003**
Model2	RMSE	0.150	0.197	0.233	0.133	0.145	0.147	0.200	0.166	**0.122**	0.137
	MAE	0.080	0.117	0.153	0.068	0.069	0.075	0.136	0.096	**0.07**	0.07
	COR	0.928	0.883	0.811	0.941	0.929	0.927	0.875	0.910	**0.95**	0.937
	BIAS	−0.025	−0.030	−0.016	−0.008	−0.006	−0.007	−0.015	−0.011	**−0.005**	−0.015
Model3	RMSE	0.132	0.179	0.232	0.133	0.135	0.119	0.172	0.166	**0.118**	0.121
	MAE	0.066	0.105	0.147	0.069	0.065	0.061	0.104	0.095	**0.061**	0.057
	COR	0.942	0.901	0.814	0.941	0.938	0.952	0.907	0.910	**0.954**	0.952
	BIAS	−0.019	−0.008	−0.016	−0.005	−0.004	0.011	−0.016	0.013	**−0.012**	0.0005
Model4	RMSE	0.129	0.177	0.234	0.133	0.126	0.116	0.167	0.167	0.117	**0.113**
	MAE	0.064	0.106	0.148	0.07	0.059	0.059	0.101	0.095	0.058	**0.056**
	COR	0.944	0.903	0.812	0.941	0.948	0.955	0.916	0.910	0.955	**0.958**
	BIAS	−0.015	0.005	−0.019	0.002	−0.007	−0.004	−0.014	0.005	−0.007	**−0.002**

The bold values in table represent the best performance case among the combination of structure and algorithm in each model

Concerning the sunshine predicting results corresponding to the without weather forecast I/O structure, we observed that in Model 1, LSTM achieved the best predicting results with RMSE of 0.192, MAE of 0.107, and correlation of 0.875. In Model 2, RNN demonstrated the best predicting results with RMSE of 0.133, MAE of 0.068, and correlation of 0.941. Concerning Model 3, RNN showed the best predicting results with RMSE of 0.133, MAE of 0.069, and correlation of 0.941. In the case of Model 4, LSTM demonstrated the best predicting results with RMSE of 0.126, MAE of 0.059, and correlation of 0.948. Therefore, overall, Model 4 reached the best predicting results. RMSE of Model 4 was 1.5 times better than that of Model 1.

Based on the sunshine predicting results using weather forecast in Model 1, LSTM achieved the best predicting results with RMSE of 0.167, MAE of 0.091, and correlation of 0.906. In Model 2, RNN showed the best predicting results with RMSE of 0.122, MAE of 0.061, and correlation of 0.954. Concerning Model 3, RNN achieved the best predicting results with RMSE of 0.118, MAE of 0.061, and correlation of 0.954. In the case of Model 4, LSTM demonstrated the best predicting results with RMSE of 0.113, MAE of 0.056, correlation of 0.958, and bias of -0.002. The experimental results indicated that Model 4 reached the best predicting performance, and RMSE of Model 4 was 1.47 times better than that of Model 1.

Figure 7 represents the graphs depicting the sunshine predicting results for DNN3 and LSTM for five days in the period of March 20-24, 2015.

In Model 1, which predicted sunshine only when incorporating meteorological factors, DNN1 exhibited large differences between the actual and predicted values, as indicated by the high RMSE of 0.269. This could be caused due to the low correlation of 0.736 and by the considerable error rate. LSTM of Model 1 demonstrated RMSE of 0.167 and the high correlation of 0.906. Accordingly, the predicted values were similar to the actual ones indicating good performance. In Model 4, DNN1 reached RMSE of 0.1161 and correlation of 0.955, and LSTM achieved a RMSE of 0.113 and correlation of 0.958. In line with the low error rates and high correlation values, these two predicting models represented no considerable differences in the graphs, and the predicted values were similar to actual ones.

Table 10 represents the solar radiation predicting results. The gray parts indicate the best results in each model. Similarly as in the sunshine predicting, the I/O structures using weather forecasts achieved acceptable solar radiation results, and LSTM demonstrated the best predicting results in every model. In Model 1, LSTM showed the best predicting results with RMSE of 0.079, MAE of 0.051, and correlation of 0.945. In Model 2, LSTM achieved the best predicting results with RMSE of 0.038, MAE of 0.022, and correlation of 0.985.

Concerning the without weather forecast I/O solar radiation predicting results, in Model 1, LSTM demonstrated the best predicting results with RMSE of 0.089, MAE of 0.054, and correlation of 0.924. In Model 2, RNN achieved the best predicting results with RMSE of 0.047, MAE of 0.025, and correlation of 0.978. Concerning Model 3, RNN achieved the

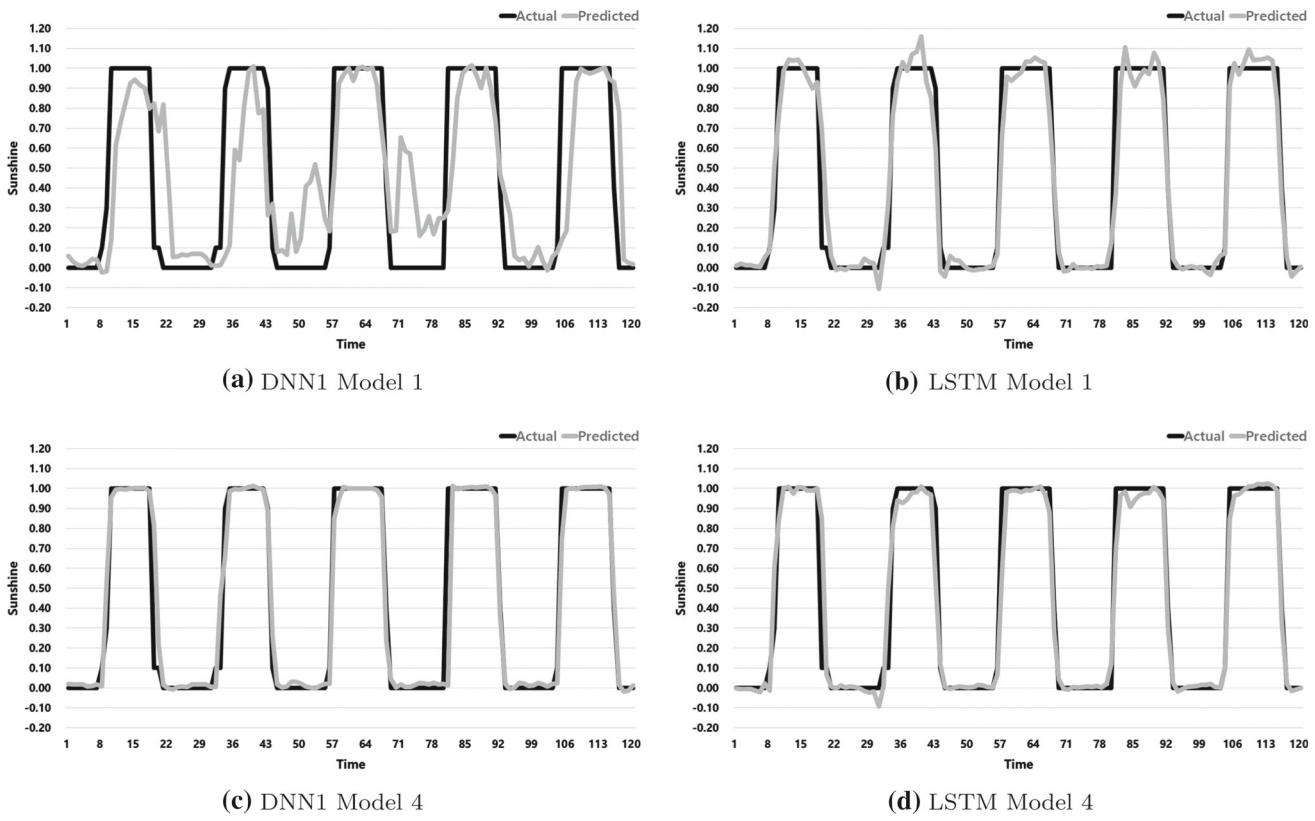

Fig. 7 Predicting results of sunshine

Table 10 Predicting results of solar radiation

		Without weather forecast I/O structure					Weather forecast I/O structure				
		DNN1	DNN2	DNN3	RNN	LSTM	DNN1	DNN2	DNN3	RNN	LSTM
Model1	RMSE	0.179	0.193	0.159	0.091	0.089	0.155	0.168	0.133	0.082	**0.079**
	MAE	0.134	0.151	0.124	0.057	0.054	0.110	0.126	0.102	0.052	**0.051**
	COR	0.635	0.608	0.734	0.918	0.924	0.749	0.743	0.838	0.939	**0.945**
	BIAS	0.039	0.031	0.021	0.012	0.012	0.021	0.024	0.025	0.019	**0.02**
Model2	RMSE	0.071	0.094	0.112	0.047	0.048	0.072	0.097	0.097	0.041	**0.038**
	MAE	0.047	0.068	0.085	0.025	0.027	0.048	0.075	0.077	0.024	**0.022**
	COR	0.949	0.925	0.874	0.978	0.978	0.945	0.915	0.909	0.983	**0.985**
	BIAS	0.012	−0.02	−0.011	0.001	−0.001	0.009	−0.001	0.009	0.002	**0.001**
Model3	RMSE	0.056	0.071	0.106	0.048	0.05	0.05	0.067	0.095	0.04	**0.04**
	MAE	0.033	0.048	0.077	0.026	0.027	0.029	0.045	0.072	0.023	**0.022**
	COR	0.971	0.954	0.888	0.977	0.974	0.974	0.960	0.918	0.984	**0.985**
	BIAS	−0.007	0.001	−0.002	0.001	0.003	0.007	0.009	0.013	0.003	**0.004**
Model4	RMSE	0.053	0.071	0.107	0.048	0.046	0.047	0.066	0.091	0.044	**0.039**
	MAE	0.029	0.048	0.079	0.027	0.024	0.028	0.045	0.068	0.027	**0.023**
	COR	0.973	0.956	0.887	0.977	0.979	0.977	0.961	0.921	0.981	**0.986**
	BIAS	−0.001	0.004	0.001	−0.003	0.002	0.012	−0.002	0.013	0.005	**0.008**

The bold values in table represent the best performance case among the combination of structure and algorithm in each model

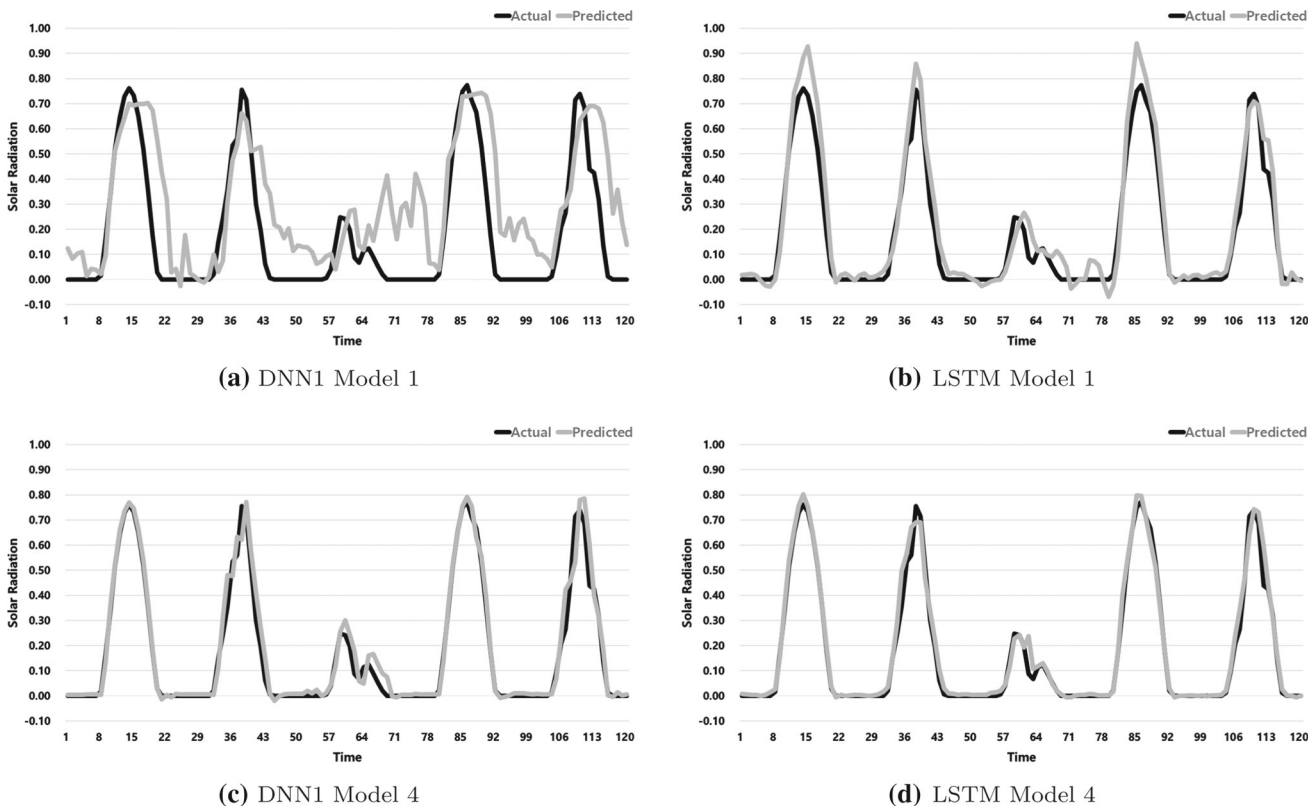

(a) DNN1 Model 1

(b) LSTM Model 1

(c) DNN1 Model 4

(d) LSTM Model 4

Fig. 8 Predicting results of solar radiation

best predicting results with RMSE of 0.048, MAE of 0.026, and correlation of 0.977. In Model 4, LSTM reached the best predicting results with RMSE of 0.046, MAE of 0.024, and correlation of 0.979. Therefore, we concluded that Model 4 achieved the best predicting results. RMSE of Model 4 was 1.8 times better than that of Model 1.

Based on the solar radiation predicting results using weather forecast in Model 1, LSTM achieved the best predicting results with RMSE of 0.079, MAE of 0.051, and correlation of 0.945. In Model 2, LSTM demonstrated the best predicting results with RMSE of 0.038, MAE of 0.022, and correlation of 0.985. In the case of Model 3, LSTM reached the best predicting results with RMSE of 0.04, MAE of 0.022, and correlation of 0.985. Concerning Model 4, LSTM showed the best predicting results with RMSE of 0.039, MAE of 0.023, and correlation of 0.986. The experimental results revealed that Model 4 achieved the best predicting results and the RMSE of Model 4 was two times better than that of Model 1. Figure 8 represents the graphs of the solar radiation predicting results for DNN and LSTM for five days in the period from March 20–24, 2015.

In Model 1, which predicted solar radiation only when incorporating meteorological factors, DNN1 demonstrated RMSE of 0.155 and correlation of 0.749. Therefore, the predicted values exhibited large differences from the actual ones. This could be caused by the low correlation rather than the high error rate. LSTM showed RMSE of 0.079 correlation of 0.945. Owing to a relatively low error rate and a high correlation, the predicted values were similar to the actual ones. In Model 4, DNN1 with the smallest error rate achieved RMSE of 0.047, and LSTM showed RMSE of 0.039. Accordingly, the predicted values of LSTM were similar to the actual ones. However, as shown in the graphs, overall, LSTM achieved better results compared with DNN.

In all predicts on sunshine and solar radiation, the predict of solar radiation demonstrated the error rates two times better than that of sunshine. Table 11 provides the predicting results for solar power generation.

Based on the power generation amount predicting results, among without weather forecast I/O structures, in Model 1, LSTM achieved the best predicting results with RMSE of 0.121, MAE of 0.086, and correlation of 0.862. In Model 2, LSTM showed the best predicting results with RMSE of 0.086, MAE of 0.047, and correlation of 0.931. Concerning Model 3, LSTM demonstrated the best predicting results with RMSE of 0.66, MAE of 0.038, and correlation of 0.941. In the case of Model 4, LSTM showed the best predicting results with RMSE of 0.064, MAE of 0.036, and correlation of 0.955. The experimental results indicated that Model 4 reached the best predicting results. The

Table 11 Predicting results of solar power generation

		Without weather forecast I/O structure					Weather forecast I/O structure				
		DNN1	DNN2	DNN3	RNN	LSTM	DNN1	DNN2	DNN3	RNN	LSTM
Model1	RMSE	0.204	0.237	0.221	0.13	0.121	0.197	0.228	0.212	0.128	**0.115**
	MAE	0.150	0.189	0.176	0.077	0.072	0.139	0.176	0.167	0.091	**0.067**
	COR	0.557	0.587	0.725	0.851	0.862	0.626	0.657	0.793	0.848	**0.876**
	BIAS	0.008	0.116	0.134	0.049	0.039	0.008	0.009	0.015	0.057	**0.037**
Model2	RMSE	0.117	0.154	0.216	0.091	0.086	0.114	0.168	0.195	0.09	**0.085**
	MAE	0.066	0.113	0.176	0.052	0.047	0.074	0.128	0.169	0.051	**0.045**
	COR	0.862	0.823	0.739	0.93	0.931	0.867	0.827	0.814	0.933	**0.935**
	BIAS	0.002	0.060	0.129	0.033	0.025	0.035	0.092	0.128	0.032	**0.025**
Model3	RMSE	0.083	0.118	0.207	0.068	0.066	0.082	0.116	0.194	0.066	**0.063**
	MAE	0.046	0.086	0.161	0.039	0.038	0.049	0.085	0.154	0.039	**0.036**
	COR	0.929	0.898	0.771	0.946	0.941	0.929	0.906	0.824	0.953	**0.955**
	BIAS	0.021	0.048	0.129	0.009	0.007	0.026	0.052	0.132	0.012	**0.011**
Model4	RMSE	0.080	0.112	0.197	0.067	0.064	0.078	0.124	0.208	0.064	**0.062**
	MAE	0.047	0.080	0.153	0.038	0.036	0.046	0.093	0.164	0.037	**0.035**
	COR	0.931	0.901	0.776	0.949	0.955	0.929	0.898	0.837	0.953	**0.958**
	BIAS	0.021	0.036	0.114	0.007	0.011	0.007	0.006	0.151	0.008	**0.009**

The bold values in table represent the best performance case among the combination of structure and algorithm in each model

RMSE of Model 4 was 1.89 times better than that of Model 1.

Among the data structures incorporating weather forecasting, in Model 1, LSTM showed the best predicting results with RMSE of 0.115, MAE of 0.067, and correlation of 0.876. In Model 2, LSTM achieved the best predicting results with RMSE of 0.085, MAE of 0.045, and correlation of 0.935. Concerning Model 3, LSTM provided the best predicting results with RMSE of 0.63, MAE of 0.062, and correlation of 0.958. In Model 4, LSTM showed the best predicting results with RMSE of 0.064, MAE of 0.036, and correlation of 0.955. The experimental results revealed that Model 4 achieved the best predicting results. The RMSE of Model 4 was 1.88 times better than that of Model 1.

Concerning the predicting results on sunshine, solar radiation, and power generation, LSTM in Model 4 showed the best experimental results. However, considering sunshine prediction in Model 3, RNN achieved better predicting results, as in the case of LSTM, the difference between the best and worst results was large, whereas for RNN, the results were stable meaning that the difference between the best and worst results was not considerable. Figure 9 presents the graphs for the DNN1, RNN, and LSTM predicting results corresponding to the power generation amounts for five days in the period October 14–18, 2015.

In Model 4, RMSE of DNN1 exhibited the smallest error rate of 0.078, and RMSE of LSTM was 0.062. Therefore, the predicted values were rather similar to actual ones. However, LSTM showed more stable results over DNN1 in terms of finding the largest and smallest power generation amounts.

The following results can be seen through all experiments such as sunshine, solar radiation, and power generation prediction.

1. In sunshine and solar radiation predictions, which have a great influence on power generation, solar radiation prediction was better than sunshine prediction.
2. More research is needed to predict sunshine.
3. Model 4, which uses more meteorological factors, has better predictive rate than Model 1.
4. The I/O structure using weather forecast had better error rates such as RMSE and MAE than the I/O structure without weather forecast.
5. The correlation was higher with better prediction rate.
6. BIAS of power generation was positive, and it can be seen that the predicted value is a little higher than the actual value.
7. If the weather forecast is correct, it is expected to help improve the predict rate up to the point of predict.

5 Conclusion

In the present study, we proposed a model for power generation prediction based on weather forecasts with prediction algorithm relied on the neuro-fuzzy and ANNs. As a result of the conducted experiment, RMSE of LSTM was 1.72

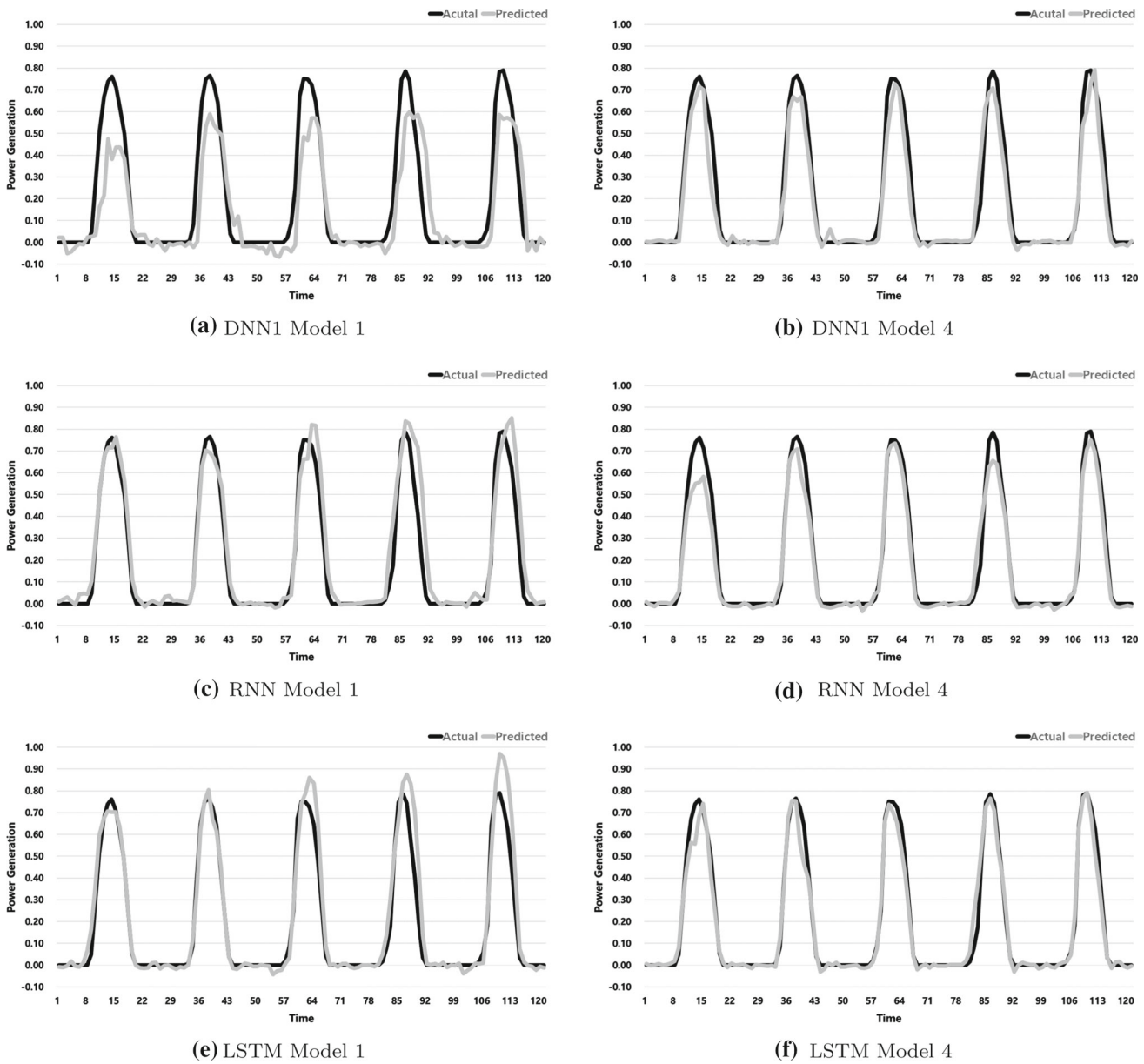

Fig. 9 Forecasting results of solar power generation

times better than ANFIS. We concluded that the prediction rate of ANNs was higher than that of the neuro-fuzzy approach. Therefore, we proposed a power generation prediction method using ANNs, such as DNN, RNN, and LSTM.

DNN was tested with 24-hr, 12-hr, and 7-hr data according to the correlation between the total amount of transportation and the amount of power generation. The 24-hr data are DNN1, the 12-hr data are DNN2, and the 7-hr data are DNN3. The experimental results revealed that the DNN1 predict was better compared with the outputs of DNN2 and DNN3, except for Model 1. It is because in DNN2 and DNN3, the correlation between power generation and cloudiness has increased, but the correlation between power generation and the rest of the fundamental weather factors, sunshine, and solar radiation has decreased.

Concerning among the ANNs, the RNN and LSTM methods were found to be more suitable for the time series structure, as they exhibited the lower error rate compared with DNN. In the RNN-LSTM test, the best result was achieved for the setting with the 24 time stamps compared with the 12 or 48 time stamps. Also, there was no difference observed in the results of the experiments on RNN-LSTM and multi-RNN-LSTM that were designed as multilayered structure.

The data structures incorporating weather forecast provided better performance in all aspects compared with those without weather forecasts. That is, in all models, the data

structure using weather forecast showed a better RMSE error rate. Model 4 that is using weather forecasts structure achieved the best results in the estimation of sunshine and solar radiation. Compared to Model 1, RMSE was reduced by 1.25 times for sunshine and by 2.03 times for solar radiation. In all experiments, the error rate associated with solar radiation was more than two times higher than that of sunshine. The solar power generation prediction was implemented based on best prediction results on the solar radiation and sunshine data among each algorithm. The experimental results indicated that the predicting outcome of Model 4 was the most accurate one, and its RMSE was 1.85 times better than that of Model 1. However, no considerable differences with the predicting results obtained using only predicted solar radiation were observed. This was because solar radiation was found to be a more important meteorological factor in the prediction of solar power generation.

In the present study, we confirmed the superiority of the solar power generation prediction approach based on ANNs over the neuro-fuzzy methods, applied to same data structure. It can be seen that the prediction model using the weather forecast proposed in this study showed better prediction performance than the prediction model without the weather forecasts. Moreover, it was demonstrated that the prediction rate improved depending on various I/O structures.

This paper suggested that it is possible to predict the amount of power generation during the weather forecast using predicted solar and solar data. In the future, the further improvement of predicting results can be realized by combining various deep learning networks and input factors.

Acknowledgements This work was supported by the Korea Institute of Energy Technology Evaluation and Planning (KETEP) and the Ministry of Trade, Industry and Energy (MOTIE) of the Republic of Korea (No. 20194030202290).

Compliance with ethical standards

Conflict of interest The authors declare that they have no conflict of interest.

Ethical approval This article does not contain any studies with animals performed by any of the authors.

References

Bengio Y (2009) Learning deep architectures for AI. Foundations and Trends in Machine Learning 2:1–127

Cha WC, Park JH, Cho UR, Kim JC (2014) Design of generation efficiency fuzzy prediction model using solar power element data. Trans Korean Inst Electr Eng 63:1423–1427

Conejo AJ, Plazas MA, Espinola R, Molina AB (2005) Day-ahead electricity price forecasting using the wavelet transform and ARIMA models. IEEE Trans Power Syst 20:1035–1042

Costa A, Crespo A, Navarro J, Lizcano G, Madsen H, Feitosa E (2008) A review on the young history of the wind power short-term prediction. Renew Sustain Energy Rev 12:1725–1744

Deng L, Yu D (2014) Deep learning: methods and applications. Found Trends Signal Process 7:197–387

Giebel G, Brownsword R, Kariniotakis G, Denhard M, Draxl C (2011) The State-of-the-art in short-term prediction of wind power a literature overview. Technical report, ANEMOS.plus, pp 1-109

Goodfellow I, Bengio Y, Courville A (2016) Deep learning. MIT press, Cambridge

Hong T, Wilson J, Xie J (2014) Long term probabilistic load forecasting and normalization with hourly information. IEEE Transactions on Smart Grid 5:456–462

Kim YH, Hwang YK, Kang TG, Jung KM (2016) LSTM language model based Korean sentence generation. J Korean Inst Commun Inf Sci 41:592–601

LeCun Y, Bengio Y, Hinton G (2015) Deep learning. Nature 521:436–444

Lee BH (2017) A study on simplified robust optimal operation of microgrids considering the uncertainty of renewable generation and loads. Trans Korean Inst Electr Eng 66:513–521

Lee CS, Ji PS (2015) Development of daily PV power forecasting models using ELM. Trans Korean Inst Electr Eng 64:164–168

Lee DJ, Lee JP, Lee CS, Lim JY, Ji PS (2015) Development of PV power prediction algorithm using adaptive neuro-fuzzy model. Trans Korean Inst Electr Eng 64:246–250

Lee SM, Lee WJ (2016) Development of a system for predicting photovoltaic power generation and detecting defects using machine learning. KIPS Trans Comput Commun Syst 5:353–360

Lei M, Shiyan L, Chuanwen J, Hongling L, Yan Z (2009) A review on the forecasting of wind speed and generated power. Renew Sustain Energy Rev 13:915–920

Mirasgedis S, Sarafidis Y, Georgopoulou E, Lalas DP, Moschovits M, Karagiannis F, Papakonstantinou D (2006) Models for mid-term electricity demand forecasting incorporating weather influences. Energy 31:208–227

Mohamed H, EL-Kader A, Ibrahim A, EL-Shora A (2020) Developing a neuro-fuzzy model for weather prediction. Int J Comput Appl 177:15–26

Priya PI, Ghosh DK, Kannan A, Ganapathy S (2014) Behaviour analysis for social networks using genetic weighted fuzzy C-means clustering and neuro-fuzzy classifier. Int J Soft Comput 9:138–142

Rhee SB, Kim KH, Lee SG (2011) Optimal operation scheme of microgrid system based on renewable energy resources. Trans Korean Inst Electr Eng 60:1467–1472

Thangaramya K, Kulothungan K, Logambigai R, Selvi M, Ganapathy S, Kannan A (2019) Computer networks energy aware cluster and neuro-fuzzy based routing algorithm for wireless sensor networks in IOT. Comput Netw 151:211–223

Welch RL, Ruffing SM, Venayagamoorthy GK (2009) Comparison of feedforward and feedback neural network architectures for short term wind speed prediction. International Joint Conference on Neural Networks, pp 3335–3340

Yona A, Senjyu T, Funabashi T, Mandal P, Kim CH (2013) Decision technique of solar radiation prediction applying recurrent neural network for short-term ahead power output of photovoltaic system. Smart Grid Renew Energy 4:32–38

Yu J, Kim S (2016) Locally-weighted polynomial neural network for daily short-term pear load forecasting. Int J Fuzzy Logic Intell Syst 16:163–172